Pakistan J. Zool., vol. 53(3), pp 1089-1098, 2021 DOI: https://dx.doi.org/10.17582/journal.pjz/20200222110209

Preliminary Assessment of a Coupled Dynamic-Energy Budget and Agent-based Model (DEB-ABM) for Predicting Individual and Population-Level Dynamics: A Case Study on Anchovy, *Engraulis japonicus*

Baochao Liao[1,2], Xiujuan Shan[2,3]* and Yunlong Chen[2,3]

[1]*Department of Mathematics and Statistics, Shandong University, Weihai, Shandong 264209, China*
[2]*Function Laboratory for Marine Fisheries Science and Food Production Processes, Qingdao National Laboratory for Marine Science and Technology, Qingdao, Shandong 266237, China*
[3]*Yellow Sea Fisheries Research Institute, Chinese Academy of Fishery Sciences, Qingdao, Shandong 266071, China*

Article Information
Received 22 February 2020
Revised [illegible] 2020
Accepted [illegible] April 2020
Available online 30 March 2021

Authors' Contribution
BL conceived and designed the study. XS arranged the data. BL and YC helped in data analysis. YC prepared the Figures. BL analyzed the data and wrote the article.

Key words
Dynamic energy budget, Agent-based model, Fishery surveys, *Engraulis japonicus*

ABSTRACT

Dynamic energy budget (DEB; also known as Kooijman–Metz DEB) theory is a well-tested framework for modelling energy acquisition, and for describing vital rates at which organisms store and use energy, such as for growth and reproduction. The coupling of a DEB with an agent-based model (generating a DEB- ABM) enables examination of the effects of environmental change at population level on a species to be examined. The present study applied a DEB-ABM to the Japanese anchovy *Engraulis japonicus*. The DEB-ABM accurately captured energy acquisition and allocation throughout the anchovy lifecycle (egg, yolk sac larva, exogenous feeding larva, juvenile, and adult), and predicted how individual-level processes affect energy dynamics at higher levels of biological organization. We estimated primary model parameters (e.g., energy conductance, $\dot{v}$; allocation efficiency, κ; and volume-specific somatic maintenance, $[\dot{p}_M]$), and for a 5-year simulation, calculated mean population growth rate (r_p) of 3.4 year^{-1}. When DEB theory is combined with an ABM, the combined model describes the dynamics of a population of individuals, where each individual follows the energy budget model. Predicted demographic rates (growth, survival, reproduction) fell within observed ranges, fit average recorded values, and captured known seasonal trends. The DEB-ABM correlated with intrinsic and density-independent population growth rates, and may be useful for predicting the metabolic responses of individuals or populations to environmental change.

INTRODUCTION

Dynamic energy budget (DEB; also known as the Kooijman–Metz DEB) theory links the physiological processes of individual organisms into a single framework (van der Meer, 2006; Kooijman, 2010). The theory describes the energy and matter fluxes within an individual, and between it and its environment (Kooijman, 2010; Marn, 2016; Agüera *et al*., 2017). Traditional DEB bioenergetic models are applied at the level of the individual, and can be used to deduce the energy input from individual-level growth and reproduction (Kooijman, 2010; Jusup *et al*., 2011; Marn, 2016; Birnir *et al*., 2018). This theory systematically describes how an organism acquires and uses energy and other physiologically essential elements (Nisbet *et al*., 2012), and provides a framework within which the effects of environmental variables, such as food density, and temperature, influence physiological performance (Jusup *et al*., 2011; Marn, 2016).

An agent-based model (ABM) predicts how individual-level processes affect energy dynamics at higher levels of biological organization (Railsback and Grimm, 2011; Martin *et al*., 2013). ABMs have been widely used to predict the performance of a given population in response to fluctuations in regional environments (Sibly *et al*., 2013). When DEB theory is coupled with an ABM, the combined model, a DEB-ABM, describes the dynamics

* Corresponding author: shanxj@ysfri.ac.cn
0030-9923/2021/0003-1089 $ 9.00/0

of a population of individuals, with each individual following an energy budget model (Railsback and Grimm, 2011; Sibly *et al.*, 2013). This combined model can be used to predict how the energy dynamics at higher levels of biological organisation emerge from individual-level processes (Sibly *et al.*, 2013). DEB models have been coupled with ABMs to study fish population dynamics in a large body of work (Martin *et al.*, 2013; Sibly *et al.*, 2013; Grossowicz *et al.*, 2017; Desforges *et al.*, 2017; Smallegange *et al.*, 2017).

The pelagic Japanese anchovy (*Engraulis japonicus*; Temminck and Schlegel, 1846) is an important prey species and plankton feeder; it is also the most abundant fish in Chinese waters, including the Bohai (BH), Yellow (YS), and East China (ECS) seas (Jin, 2004; Wang *et al.*, 2003). However, increased fishing effort in Chinese waters in recent decades has led to dramatic changes in the population structure of the anchovy fishery. This small, rapidly reproducing fish has a life span of approximately 4 years (Iversen *et al.*, 1993); it acquires a portion of its reproductive energy reserves during a productive period a few months before spawning season (Zhao *et al.*, 2003; Zhao *et al.*, 2008). Individuals grow rapidly during their first year, and mature after their first winter (Zhu and Iversen, 1990; Chiu and Chen, 2001). Their life-cyc includes five stages: egg, yolk sac larva, exogenou feeding larva, juvenile, and adult (Wan and Bi 2012; Wang *et al.*, 2003).

In this present study, the DEB-ABM m l zed the contributions of different energy rces and lculated the energy budget required to ma tain gro h and reproduction of a small and apidly re ducing species *E. japonicus* in Chinese as. Our aims a e to: i) find a parameterized method an validation of model output; (ii) present a no odel investigating the dynamic population-le ene y budg of anchovy; and iii) determine the m quantitative variable to explain energy budgets re vant to growth and reproduction of anchovies across stu y areas.

MATERIALS AND METHODS

Data collection

The study area included the regions YS-1 (33° 30′–37° 00′ N, 129° 00′–124° 00′ E) and YS-2 (32° 00′–39° 00′ N, 121° 00′–125° 00′ E). Data on spawning adults were collected every May (peak anchovy spawning season), from 2000 to 2004, as part of the pelagic acoustic surveys undertaken by the Chinese-Norwegian "BeiDou" project (Wan and Bian, 2012). Fishery surveys were conducted in three anchovy spawning grounds: the south of the Shandong Peninsula (in Laizhou Bay of the BS), the YS, and the coastal waters of the ECS (Zhao, 2006; Zhu *et al.*, 2007; Wan and Bian, 2012; Wang *et al.*, 2003). In the YS, adult anchovies spawn between May and September, with spawning peaking in May–June (Zhinan *et al.*, 2002; Wang *et al.*, 2003). Individual-level data on length, weight, and age are available for the period 2000–2004 (Kim *et al.*, 2005; Zhao, 2006; Zhu *et al.*, 2007; Wan and Bian, 2012; Wang *et al.*, 2003). Satellite-derived sea surface water temperatures were obtained from the International Research Institute for Climate Prediction (IRI/LDEO) Climate Data Library (Wang *et al.*, 2003; Shan *et al.*, 2017).

Individual-level

The DEB model predicts ividua nergy allocation, acquisition, and use r gr th a reproduction (Kooijman, 2010; Ni et al., 2 12) ood intake was controlled by a scale dim sionless and Holling type-II) functional fee g resp se (f) rve that ranged between 0 (i.e., no f d ntake) an i.e., maximum food intake); a fixed fraction of κ was allocated to maintenance and gr th, and the re ining energy ($1-\kappa$) was utilized for de elopment and reproduction (Table I). The food uptake wa roport nal to the surface area of the larva and to food densi ingestion rate was equal to $\dot{p}_X = f(X)^* \{\dot{p}_X\}^* V^{2/3}$, here $f(X)=X/(X+K)$. The four state variables (fluxes, units: J day^{-1}), including the Arrhenius temperature (T_A); the volume-specific somatic maintenance ($[\dot{p}_M]$); energy conductance ($\dot{v}$); allocation coefficient (κ); fraction of energy allocated to fixed growth (κ_G); and maturity maintenance rate coefficient (κ_J). DEB dictated that energy is assimilated ($\dot{p}_A$) from food and transferred into reserve (E). The fixed fractions (κ and $1-\kappa$) of the catabolized energy ($\dot{p}_C$) are allocated to either soma (E_v, units: J) or maturation/reproduction (E_R). Increases in anchovy size (V) regulated transitions between developmental stages. All energy allocated to the reproductive buffer before puberty ($V<V_p$) was lost to maturation ($E_R=0$). DEB model was parameterized based on the biometric data of juveniles and adult *E. japonicus* (SL range: 5.8–17.2 cm) collected between 2001 and 2004 (Wan *et al.*, 2004; Zhao, 2006). Anchovy water mass W_{ww} was predicted by the following equation: $W_{ww} = \exp(-3.19+0.38^*l + 0.59^* \log(e) - 0.035^*l^* \log(e))$; this length-weight relationship is typically expressed as $W = a \times L^b$. Larval growth data were consisted of individual specimens (Total length: 1.8–5.4 cm; W_{ww}: 0.018–1.32 g). Larval growth and proximate composition data for anchovies were used to estimate the values of the state variables as follows: $E_{R0}=0$ J; $E_{GAM0}=0$ J; $E_0=0.11$ J; $E_{V0}=0.025$ J; and $V_0=0.00013$ cm^3. We set the length- and weight-at-first-feeding (day 4) values to 0.292 cm and 0.031 g, respectively (Wan *et al.*, 2002; Wan and Bian,

2012). The relationship between water temperature T and egg development time D for the anchovy was expressed as $D = 1788.42(T\text{-}273)^{-2.29}$. The DEB model parameter values are summarized in Table II.

Table I. Equations of the dynamic energy budget model fluxes and model output variables. All parameter values listed in Table II, and a conceptual diagram is shown in Kooijman 2010.

Formula	Description	Type (/units)
$\dot{p}_A = \{\dot{p}_{AM}\} \cdot f \cdot V^{2/3} with \{\dot{p}_{AM}\} = \{\dot{p}_{XM}\} ae$	Assimilation	Fluxes (J d^{-1})
$\dot{p}_C = \frac{[E]}{[E_G] + \kappa[E]} \left(\frac{[E_G]\{\dot{p}_{AM}\} V^{2/3}}{[E_m]} + [\dot{p}_M] V \right)$	Catabolic utilization	Fluxes (J d^{-1})
$\dot{p}_G = \kappa \dot{p}_C - \dot{p}_M$	Growth	Fluxes (J d^{-1})
$\dot{p}_M = [\dot{p}_M] V$	Somatic maintenance	Fluxes (J d^{-1})
$\dot{p}_R = (1-\kappa)\dot{p}_C - \dot{p}_J$	Reproduction	Fluxes (J d^{-1})
$\dot{p}_J = \min\left(\frac{1-\kappa}{\kappa} \cdot [\dot{p}_M] V, \frac{1-\kappa}{\kappa} \cdot [\dot{p}_M] V_p \right)$	Maturity maintenance	Fluxes (J d^{-1})
$\dot{p}_G = \kappa \dot{p}_C - \dot{p}_M$	Gamete allocation (synthesis)	Fluxes (J d^{-1})
$\dot{p}_{R2} = E_R \left(\frac{\{\dot{p}_{AM}\}}{[E_m] V^{1/3}} + \frac{[\dot{p}_M]}{[E_G]} \right) (1-\kappa) \frac{E}{[E_m] V + E}$ $if SST(t) > TR, else = 0$	Gamete (energy mobilization)	Fluxes (J d^{-1})
$\dot{p}_{M2} = \min(\dot{p}_M - \kappa \dot{p}_C, \dot{p}$	Emergency somatic maintenance	Fluxes (J d^{-1})
$\dot{p}_{M3} = \max(\dot{p}_M - \kappa \dot{p}_C + \dot{p}_{M2}), [E_G], 0)$	Atresia (gonad resorption)	Fluxes (J d^{-1})
$L = V^{1/3} / \ldots$ larva $\ldots$ else $V \ldots$ adults $if\ V > V_{morph}$	Total length (L)	Model output (cm)
$W_{dw} = E_V / \ldots + ((E_R + E)/\mu_E)(E_{GAM}/\mu_G)$	Total dry weight (W_{dw})	Model output (g)
$W_{ww} = W_{dw} \cdot \gamma$	Total wet weight (W_{ww})	Model output (g)
$W_{GON} = (0.015 E_V / \mu_V + E_{GAM} / \mu_G) \cdot \gamma$	Gonad weight (W_{GON})	Model output (g)
$Ed = \frac{(E_V + E + E_R + E_{GAM})}{W_{dw} (or W_{ww})}$	Energy density (E_d)	Model output (J g^{-1})
$K_{ful} = 100 W_{ww} / L^3$	Condition index (K_{ful})	Model output (g cm^3)
$GSI = W_{GON} \times 100 / W_{ww}$	Gonad somatic index (GSI)	Model output (–)

Table II. List of parameter values of the dynamic energy budget model for anchovy, *Engraulis japonicus*.

Parameters	Symbol	Definition	Unit
Max. assimilation rate	$\dot{p}_{AM}$	Feeding parameter	J cm^{-2} d^{-1}
Assimilation efficiency	ae	Feeding parameter	Dimensionless
Volume specific cost for structure	E_G	Energetic parameter	J cm^{-3}
Volume specific maintenance cost	$\dot{p}_M$	Energetic parameter	J cm^{-2} d^{-1}
Fraction of energy allocated to growth	κ	Energetic parameter	Dimensionless
Max. storage rate	E_m	Energetic parameter	J cm^{-3}
Maturity maintenance rate coefficient	$\dot{k}_j$	Maturity coefficient	d^{-1}
Maturity threshold at birth	H_B	Maturity coefficient	J
Maturity threshold at puberty	H_P	Maturity coefficient	J
Half saturation coefficient for food	K_F	Saturation coefficient	g cm^{-3}
Fraction of energy fixed into eggs	K_R	Saturation coefficient	Dimensionless
Energy conductance	$\dot{v}$	Energy conductance	cm d^{-1}
Auxiliary and compound parameters			
Size at first feeding	l_b	4.1	mm
Size at metamorphosis	l_j	4.1	cm
Energy in reserve at first feeding	E_b	0.11	J
Energy of eggs	E_0	2.66	J eggs^{-1}
Relative batch fecundity	R_{bF}	478.9	eggs g^{-1}
Spawning frequency	$\dot{S}_f$	0.3	d^{-1}
Shape coefficient (early larva)	δ_b	Estimate	Dimensionless
Acceleration factor (larvae)	f_{acc}	Estimate	Dimensionless
Density of structure	d_v	Estimate	g cm^{-3}
Energy density of structure	ρ_v	Estimate	J g^{-1}
Energy density of reserve		Estimate	J g^{-1}
Energy density of reproduction reserve	ρ_R	Estimate	J g^{-1}
Energy density of gametes	ρ_C	23880	J g^{-1}

Population-level

Population-level dynamics describe those of a population of individuals, where each individual follows an energy budget model (Martin *et al.*, 2013; Sibly *et al.*, 2013). The *i*-state model follow DEB characteristics in their size (V), reproductive output (E_R, E_{GAM}, and E_{batch}), and energy reserves (E) (Pecquerie *et al.*, 2009Sibly *et al.*, 2013; Grossowicz *et al.*, 2017), as follows:

$$\frac{d}{dt}E = \dot{p}_A - \dot{p}_C, \text{ Reserve, E}$$

$$\frac{d}{dt}V = \dot{p}_A / [E_G], \text{ Structure, } V(cm^3)$$

$$\frac{d}{dt}E_R = \dot{p}_R - \dot{p}_{R2} \quad if \quad V > V_P, \quad else = 0; \text{ with } E_V = \rho v dv V;$$

$$\frac{d}{dt}E_{GAM} = \dot{p}_{CAM} - \dot{p}_{M3} - E^*_{batch}, \text{ Gametes, } E_{GAM}$$

$$\frac{dN_i}{dt} = -h_i \cdot N_i - m_i N_i, \quad (\text{ind d}^{-1})$$

$$S = \sum_i N_i \cdot WT_i$$

$$P = \sum_i h_i N_i \cdot WT_i$$

$$N = \sum_i N_i$$

Where the variables V_i, E_i, R_i, L_i, and WT_i were associated with cohort i and simulated with DEB equations; h_i represented the harvest rate coefficient; m_i was the natural mortality rate coefficient; N_i was the number of individuals in cohort i; P was the cumulative harvest of cohorts; N was the total number of individuals; and S was the weight of all cohorts after summation to estimate the standing stock at each time step. The total recruitment (R) was calculated as a function of spawning stock biomass (SSB) (Zhao *et al.*, 2003). The characterized state variables of the individual were included reserves (E), structure (V and E_v), reproduction (E_R), and gametes (E_{GAM}; Table I) (Regner, 1996; Boussouar *et al.*, 2001). The sensitivities of the intrinsic model-specific parameters (deterministic, nondeterministic, positive, and negatively correlated) were investigated using a traditional one-parameter-at-a-time analysis (OPAT), in which each model parameter was varied separately with ±10% white noise (CV). We calculated a relative estimate error (REE) to compare results among CVs (Chen *et al.*, 2010). The REE was

evaluated by calculating a simple sensitivity index (SSI) as follows:

$$SSI_1 = \sum_{i=1}^{k} (|W_t^0 - W_t^1| / kW_t^0) * 100\ \%$$

$$SSI_2 = \frac{1}{k} \sum_{i=1}^{k} (|L_t^0 - L_t^1| / L_t^0) * 100\ \%$$

Where W_t^0 is the total estimated wet body weight in simulation (predicted with the new parameter value at time t); W_t^1 is the total actual wet body weight in simulation (predicted with the standard simulation at time t); k is the number of simulated days; L_t^0 is the total body length (predicted with the new parameter value at time t); and L_t^1 is the total body length (predicted with the standard simulation at time t). The effects of external factors, including sea surface temperature (SST), natural mortality (N_0), and food availability (X), on the growth rate of individual anchovies (or anchovy populations) was evaluated using a number of scenario-based simulations.

RESULTS

Individual traits

The Arrhenius temperature (T_A) is an expression of the effects of temperature on biological reaction rates. Here, we obtained a mean T_A value of 9800 ± 835 K, which was determined by plotting ln(1/D) against 1/T, where D and T are egg development time and temperature, respectively. We estimated two different Arrhenius relationships for the moving average (MA) of ingestion rate and respiration rate (Fig. 1). The average length- and weight-at-age of an individual anchovy collected in May predicted by our simulation were consistent with the actual length- and weight-at-age recorded during the same period by our surveys (2000–2004). We calculated energy density as the ratio of the total energy reserves to the total anchovy wet weight. By simulating differences in hatching dates in a seasonal environment, over several years, our model produced variability in anchovy body length and weight (Fig. 2). To convert state variables into units of weight (gW_{dw}), we used separate conversion factors for structures (E_V; μ_V = 19.9 KJ g^{-1}), reserves (E and E_R; μ_E = 35.2 KJ g^{-1}), and gametes (E_{GAM}; μ_G = 32 KJ g^{-1}). As anchovies have different shapes as juveniles and adults, separate shape coefficients were estimated by fitting the weight-length relationship as $W_{ww} = L^{1/3}$/L. The coefficients δ_{Adult} and δ_{larvae} were 0.169 and 0.14, respectively. The threshold structural volumes at first feeding (V_{ab}), at metamorphosis (V_{morph}), and at puberty (V_p) were estimated to be 0.000164, 0.53 and 5.43 cm^3, respectively. The simulation was designed to validate the predictions of our model under conditions of prolonged starvation. The shape coefficient δ_m was calculated as 0.172, and the scaled reserve to mass conversion $\{\dot{p}_{AM}\}/\rho_E$ was calculated as $\{\dot{p}_{AM}\}/\rho_E$ = 0.00275 cm^{-2} day^{-1}. The life-stage specific variables for the anchovy DEB-ABM are shown in Table III.

Table III. Life stage-specific variables for the anchovy dynamic energy budget–agent-based model, including mortality rates (M), temperature, scaled functional response (f), and size thresholds (L_{max}).

	Food (mg m^{-3})					f
	X	a	ω	K	Prey	
Yolk sac larvae		0	–	0	–	0
Early larvae	0.4	0.246	365	0.092	< 0.2 mm	0.65–0.85
Late larvae	0.41	0.247	355	0.092	< 0.2 mm	0.65–0.85
Juveniles	42	17	345	8.6	0.2–0.5 mm	0.6–0.8
Adults	126	92	330	34	> 0.5 mm	0.45–0.9

	L_{max} (cm)	A_{max} (d)[a]	M (d^{-1})	Temperature (℃)		
				T_{mean}	a	ω
Yolk sac larvae	0.31	4	0.621	18.5	4	238
Early larvae	3.75	40	0.285	18	4	236
Late larvae	5	80	0.053	17.5	4	232
Juveniles	10.3	280	0.004	17	3	224
Adults	14.5	1460	0.003	16	2	210

Sinusoidal functions were applied using the equation $T(t) = T_{mean} + a \sin(2\pi(t + \omega)/365)$, $X(t) = X_{mean} + a \sin(2\pi(t+\omega)/365)$, where X_{mean} or T_{mean} is the mean value, a is the amplitude, and ω is the phase shift of the sinusoid curve. For larvae, prey consists of phytoplankton sized <0.2 mm, juveniles feed on small zooplankton sized 0.2–0.5 mm, and adults feed on large mesoplankton consisting of zooplankton sized >0.5 mm. A_{max} is the given maximum age for five stages; M = 1 at the end of age-4 (1825 days).

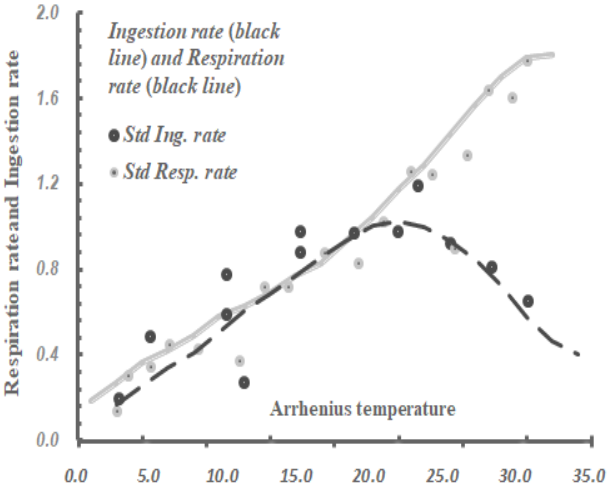

Fig. 1. Arrhenius relationships used to estimate ingestion rate (black line) and respiration rate (grey line); corrections given for temperatures from 3-32 °C.

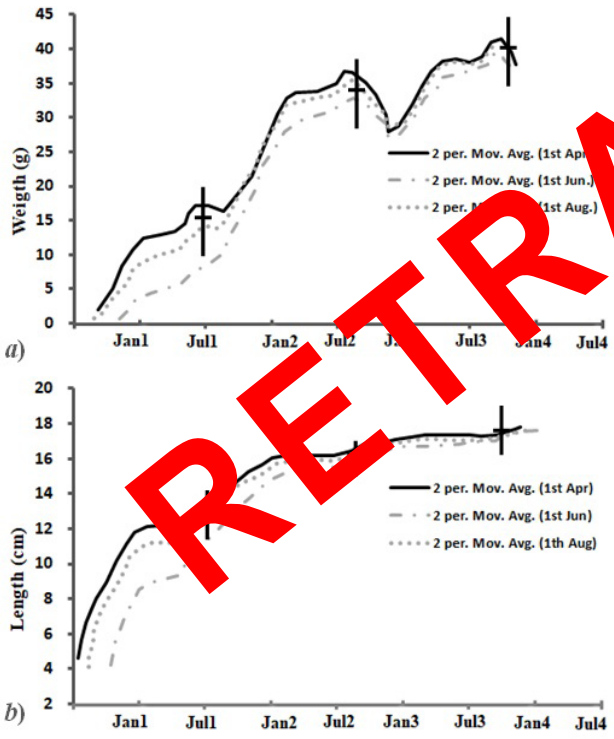

Fig. 2. Anchovy growth in weight (top panel) and -length (bottom panel) measured by simulations in hatching dates (May to September) from 2000-2004.

Population traits

In a 5-year simulation, we yielded a mean population (log-transformed biomass) growth rate (r_p) estimate of 3.4 year^{-1}. On the basis of a comparison of individual and population-level processes, the present study found that the sensitivities of age-specific annual fecundity and population rates to short-term environmental scenarios were similar. The simulation was designed to validate the predictions of the ABM (details of the anchovy ABM variables are shown in Table IV. By simulating multiple cohorts in an ABM, inter-individual variability in growth trajectories and reproductive potential became apparent. Age class 1 anchovies accounted for 30%−60% of the spawning stock; age class 2 accounted for 20%−50%, age class 3 accounted for 10%−30%, and age class 4 accounted for less than 10%. Our model produced a pattern of biphasic growth when we varied food availability during the first stage of the [illegible] life cycle. Long-term simulations were perfo[illegible]ed un[illegible] different annual environmental conditi[illegible] and h[illegible]hing [illegible]tes for length-at-age and weight-at-[illegible].

D[illegible]CU[illegible]ION

The DEB [illegible]odel describes vital rates at which o[illegible]anisms acquire [illegible]nd use energy for various activities, b[illegible] it doe[illegible]not model energy allocation or growth at the po[illegible]latio[illegible]evel (Sibly *et al.*, 2013; Grossowicz *et al.*, 2017). [illegible] combined DEB-ABM can, however, describe [illegible] dynamics of a population of individuals, where each individual follows an energy budget model (van der Meer, 2006; Kooijman, 2010). Therefore, an understanding of individual-level strategies is critical to determining the relationship between growth and time at a population level (Serpa *et al.*, 2013; Gelman *et al.*, 2014). The coupling of a DEB and ABM represents a promising method for prediction of population-level dynamics of species using individual data (Sibly *et al.*, 2013).

We used simulations to predict the effects of SST and individual fish length on use of reproductive reserves for growth (Pethybridge *et al.*, 2013; Sibly *et al.*, 2013). During the spawning season, anchovy in age classes 2 and 3 lost an average of 25% of their weight, but those in age class 1, which remained in a phase of rapid growth, did not. Length growth rates were highest for larvae (0.55–0.84 mm d^{-1}), followed by juveniles (0.10–0.55 mm d^{-1}). In age class 1 anchovies, most length and weight increases occurred between early spring and autumn, and length size increases decreased during the second year, between spring and summer. Overwinter decreases in E_D were more significant for older fish than they were for younger fish, due to the increased cost of maintenance for larger fish. Parameterization for the anchovy model was conducted at the individual level to enable prediction of population-level effects or a wide range of environmental conditions (Pethybridge *et al.*, 2013).

Table IV. List of parameters for the agent-based model for anchovy (*Engraulis japonicus*).

Symbol	Value	Unity	Variable
k_C	1.57×10^{-6}	Dimensionless	The intercept of the maximum consumption rate function
τc	-0.256	Dimensionless	The slope of the maximum consumption rate function
(T_{1C}, T_{2C}, T_{3C}, T_{4C})= (12, 15, 20, 30)		$°C_{1\times4}$	Temperature value for x_{1C}, x_{2C}, x_{3C}, and x_{4C}
(k_{S0}, k_{S1}, k_{S2}, k_{S3}, k_{S4})=(0.125, 0.175, 0.175, 0.175, 0.175)		Dimensionless	Coefficient for specific dynamic actionfor the age-0, age-1, age-2, age-3, and age-4, i.e., (k_{S0}, k_{S1}, k_{S2}, k_{S3}, k_{S4})
(k_{Eg0}, k_{Eg1}, k_{Eg2}, k_{EG3}, k_{Eg4})= (0.125, 0.160, 0.160, 0.160, 0.160)		Dimensionless	Proportion of consumed food egested for the age-0, age-1, age-2, age-3, and age-4, i.e., (k_{Eg0}, k_{Eg1}, k_{Eg2}, k_{EG3}, k_{Eg4})
(x_{1f}, x_{2f}, x_{3f}, x_{4f})$_{4\times12}$ =(7,7,7,7,7,9,12,12,12,12,7,7; 11,11, 11,12,13,14,20,20,20,20,11,11; 13,13,13,14,16,17,26,26,26,26,13,13; 15,15,15,16,18,21,30,30,30,30,15,15)		$°C_{4\times12}$	Temperature value (i.e., x_{1f}, x_{2f}, x_{3f}, and x_{4f}) for the fitness function corresponding to four temperatures, T_{1C}, T_{2C}, T_{3C}, and T_{4C}, in 12 months, respectively
(x_{1C}, x_{2C}, x_{3C}, x_{4C})= (0.1, 0.9, 0.9, 0.1)		Dimensionless	Proportion of the maximum consumption rate (C_{max}) at x_{1C}, x_{2C}, x_{3C} and x_{4C}
a_s	151.1	Dimensionless	The non-dimensional parameter in *R-SSB* model
b_s	0.299	Dimensionless	The non-dimensional parameters in *R-SSB* model

The $g(P)$ is a function expressed by $g(P) = (\Sigma P_i v_i/K)/(1 + (\Sigma P_i v_i/K))$; i denotes the prey type $I = 1$–3; K is the half-saturation constant; $h(T) = g_{Tc1}\times g_{Tc2}$, $g_{Tc1} = (x_{1C} * t^*)/(1+ x_{1C}(t^*-1))$; and $g_{Tc1} = x_{4C} * t^{\#})/(1+x_{4C}(t^{\#}-1))$, where x_{1C}, x_{2C}, x_{3C}, and x_{4C} are the values of the C_{max} function corresponding to four temperatures, T_{1C}, T_{2C}, T_{3C}, and T_{4C}, respectively; x_{1f}, x_{2f}, x_{3f}, and x_{4f} are the values of the fitness function corresponding to four temperatures, respectively; $t^* = \exp\{[1/(T_{2C} - T_{1C})]*(T- T_{1C})\} *[x_{2C}(1- x_{1C})]/[x_{1C}(1- x_{1C})]$; and $t^{\#} = \exp\{[1/(T_{4C} - T_{3C})]*(T- T_{3C})\}*[x_{4C}(1- x_{3C})]/ [x_{4C}(1- x_{3C})]$. Special dynamic action (S) represents the energy allocated to the food digestive process: $S = k_S(C-E_g)$; and egestion (E_G) is a constant proportion of consumption; $E_g = k_{Eg}C$, where k_S is the proportion of assimilated energy lost to special dynamic action, and k_{Eg} is the scaling factors for egestion (Jin, 2004; Wang *et al*., 2003).

For the population-level ABM, relatively simple responses emerged from complex individual processes (Sibly *et al*., 2013). Population-level biomass and daily production varied with season, coinciding with numerical abundance. The length size of an individual often affects its survival, chance of reproduction, growth, and number and size of its offspring (Zuidema *et al*., 2010). In a 5-year simulation under standard environmental conditions, our model estimated a mean anchovy population (log-transformed biomass) growth rate (r_p) of 3.4 year^{-1}.

Many species have complex life cycles, with individuals at different stages classified by different attributes- e.g. plant populations have long-living seed banks, and an additional discrete-state variable is thus required to keep track of seed numbers (Ellner and Rees, 2006; Zuidema *et al*., 2010). After simulating multiple cohorts, inter-individual variations in reproductive potential due to inter-annual variability in environmental conditions became apparent. Intra-specific variation in population size was high during the first year and thereafter decreased with age. Using the DEB-ABM, we can begin to observe the action of population size and structure at the level of the individual. Similar observations, including population-level empirical generaliations, may be obtained once energy budget models are more routinely used in ABMs.

The DEB-ABM model explained many anchovy life history parameters well, including age-at-maturity, spawning interval, batch fecundity, seasonal fecundity, and condition dynamics. It increases our understanding of Yellow Sea anchovy reproductive strategies. Predicted feeding rates as a proportion of body weight are consistent with estimates based on stomach content (2.5%–4%) reported by Sun *et al*. (2006). Predicted inter-spawning intervals at peak spawning season are within ranges typically given for anchovies (3–5 days). Individual growth of anchovy results from the integration of a series of processes, such as growth, reproduction, maturation, and activity (Celisse, 2008). Formultiple-batch spawners, the level of energy reserves available for reproduction determines the number of egg batches an individual will spawn (Jager and Klok, 2010).

CONCLUSION

This modelling approach, “the coupling of an ABM with DEB theory”, captured the acquisition/allocation of energy throughout the anchovy lifecycle. For a 5-year simulation, we calculated the mean population growth rate (r_p) to be 3.4 year^{-1}. The primary parameters [$\dot{p}_M$], [E_G], and [E_M] were estimated at 48 J cm^{-3} day^{-1}, 4,000 J cm^{-3}, and 2,700 J cm^{-3}, respectively. The population-level simulation was initialised with one cohort, consisting of one yolk–sac larva. The stage durations of individual traits are dependent on two forcing variables: SST and food density. The present study serves as a basis for further

analyses of anchovy population health in the northwest Pacific Ocean.

ACKNOWLEDGEMENTS

This study was funded by the National Key R&D Program of China (Grant no. 2017YFE0104400), National Basic Research Program of China (grant number 2015CB453303), the Joint Funds of the National Natural Science Foundation of China (grant number U1806202), AoShan Talents Cultivation Program Supported by Qingdao National Laboratory for MarinemScience and Technology (2017ASTCP-ES07) and the Research Program Supported by Laboratory for Marine Fisheries Science and Food Production Processes, Qingdao National Laboratory for Marine Science and Technology, China (grant number 2016LMFS-B14). The authors thank Dr Yan Jiao, Dr Kui Zhang, Dr Yongjiu Feng and Dr Lisha Guan for sharing their expertise on the research. Specifically, we thank the Dr Jacob Johansen, Steve O'Shea and Andrew Bullen for their assistance on earlier drafts of the manuscript, and the two anonymous reviewers for their many helpful comments.

Statement of conflict of interest

The authors have declared no conflict of interest.

REFERENCES

Agüera, A., Ahn, I.Y., Guillaumot, C., [illegible] and De-Hua, W., 2017. A Dynamic Energy Budget (DEB) model to describe [illegible] (King, 1832) seasonal feeding and metabolism. *PLoS One*, **12**: e0183848. https://doi.org/10.1371/journal.pone.0183848

Birnir, B., Ca[illegible]A., C[illegible]rián [illegible] and Vidal, P., 2018. Dynamic energy budget approach to evaluate antibiotic effects on biofilms. *Commun. Nonlin. Sci. Num. Simul.*, **54**: 70-83. https://doi.org/10.1016/j.cnsns.2017.[illegible]016

Bolker, B.M., 2008. *Ecological models and data in R*. Princeton University Press, pp.114-216. https://doi.org/10.1515/9781400840908

Boussouar, A., Le Bihan, S., Arino, O. and Prouzet, P., 2001. Mathematical model and numerical simulations of the migration and growth of Biscay Bay anchovy early larval stages. *Oceanol. Acta*, **24**: 489–504. https://doi.org/10.1016/S0399-1784(01)01167-7

Celisse, A., 2008. *Model selection via cross-validation in density estimation, regression, and change-points detection.* Doctoral dissertation, Université Paris Sud-Paris XI.

Chen, C.S., Tzeng, C.H. and Chiu, T.S., 2010. Morphological and molecular analyses reveal separations among spatiotemporal populations of anchovy (*Engraulis japonicus*) in the southern East China Sea. *Zool. Stud.,* **49**: 270-282.

Chiu, T.S. and Chen, C.S., 2001. Growth and temporal variation of two Japanese anchovy cohorts during their recruitment to the East China Sea. *Fish. Res*., **53**: 1-15. https://doi.org/10.1016/S0165-7836(00)00294-0

Desforges, J.P.W., Sonne, C. and Dietz, R., 2017. Using energy budgets to combine ecology and toxicology in a mammalian sentinel species. *Scient. Rep*., **7**: srep46267. https://doi.org/10.1038/srep46267

Ellner, S.P. and Rees, M., 2006. Integral projection models for species with complex demography. *Am. Nat.*, **167**: 410-428. https://doi.org/10.1086/[illegible]

Gelman, A., Hwang, J. and Vehtari, A., 2014. Understanding predictive information criteria for Bayesian models. *Stat. Comput*., **24**: 997-1016. https://doi.org/10.1007/s11222-013-9416-2

Grossowicz, M., Marques, G.M. and Voorn, G.A.K.V., 2017. A dynamic energy budget (deb) model to describe population dynamics of the marine cyanobacterium prochlorococcus marinus. *Ecol. Model*., **359**: 320-332. https://doi.org/10.1016/j.ecolmodel.2017.06.011

Hao, W., Jian, S., Ruijing, W., Lei, W. and Yi'an, L., 2003. Tidal front and the convergence of anchovy (*Engraulis japonicus*) eggs in the yellow sea fish. *Oceanography,* **12**: 434-442. https://doi.org/10.1046/j.1365-2419.2003.00259.x

Iseki, K. and Kiyomoto, Y., 1997. Distribution and settling of Japanese anchovy (*Engraulis japonicus*) eggs at the spawning ground off Changjiang River in the East China Sea. *Fish. Oceanogr*., **6**: 205-210. https://doi.org/10.1046/j.1365-2419.1997.00040.x

Iversen, S.A., Zhu, D., Johannessen, A. and Toresen, R., 1993. Stock size, distribution and biology of anchovy in the Yellow Sea and East China Sea. *Fish. Res*., **16**: 147-163. https://doi.org/10.1016/0165-7836(93)90049-D

Jager, T. and Klok, C., 2010. Extrapolating toxic effects on individuals to the population level: the role of dynamic energy budgets. *Philos. Trans. R. Soc. London B: Biol. Sci*., **365**: 3531-3540. https://doi.org/10.1098/rstb.2010.0137

Jin, X., 2004. Long-term changes in fish community structure in the Bohai Sea, China. *Estuar. Coast. Shelf. Sci*., **59**: 163-171. https://doi.org/10.1016/j.

ecss.2003.08.005

Jiang, Y.Y. and Zhuang, Z.M., 2005. Mitochondrial DNA sequence variation of Japanese anchovy *Engraulis japonicus* from the Yellow Sea and East China Sea. *Fish. Sci.*, **71**: 299-307. https://doi.org/10.1111/j.1444-2906.2005.00964.x

Jin, X.S., Johannes, H., Zhao, X.Y. and Li, F.G., 2001. Study on the quota management of anchovy (*Engraulis japonicus*) in the Yellow Sea. *J. Fish. Sci. China*, **8**: 27-30.

Jin, X. and Tang, Q., 1996. Changes in fish species diversity and dominant species composition in the Yellow Sea. *Fish. Res.*, **26**: 337-352. https://doi.org/10.1016/0165-7836(95)00422-X

Jusup, M., Klanjscek, T., Matsuda, H. and Kooijman, S.A.L.M., 2011. A full lifecycle bioenergetic model for bluefin tuna. *PLoS One*, **6**: e21903. https://doi.org/10.1371/journal.pone.0021903

Kim, J.Y., Kang, Y.S., Oh, H.J., Suh, Y.S. and Hwang, J.D., 2005. Spatial distribution of early life stages of anchovy (*Engraulis japonicus*) and hairtail (*Trichiurus lepturus*) and their relationship with oceanographic features of the East China Sea during the 1997–1998 El Niño Event. *Estuar., Coast. Shelf. Sci.*, **63**: 13-21. https://doi.org/10.1016/ecss.2004.10.002

Kooijman, S.A.L.M., 2010. *Dynamic energy budgets theory for metabolic organization*, d edition. Cambridge University Press, Great Br in.

Lin, L., Zhu, L., Liu, S.F., Su, Y.Q. an huang, Z M., 2011. Polymorphic microsatellite oc for the anese anchovy *Engraulis jap icus* (*Eng ulidae*). *Genet. mol. Res.*, **10**: 76 768. https://d org/10.4238/vol10-2gmr1085

Lika, K., Kearne R., F tas, J van der Veer, H.W., van der eer, , Wijs , J.W. and Kooijman, S.A., 201 T ariation method for estimating the parame of the standard dynamic energy budget mode I: Philosophy and approach. *J. Sea Res.*, **66**: 270-277. https://doi.org/10.1016/j.seares.2011.07.010

van der Meer, J., 2006. An introduction to Dynamic Energy Budget (DEB) models with special emphasis on parameter estimation. *J. Sea Res.*, **56**: 85-102. https://doi.org/10.1016/j.seares.2006.03.001

Maley, C.C. and Caswell, H., 1993. Implementing I-state configuration models for population dynamics: An object-oriented programming approach. *Ecol. Model.*, **68**: 75–89. https://doi.org/10.1016/0304-3800(93)90109-6

Marn, N., 2016. *Life cycle and ecology of the loggerhead turtle (Caretta caretta, Linnaeus, 1758): development and application of the Dynamic Energy Budget model*. Ph.D. thesis. Amsterdam University.

Martin, B.T., Jager, T., Nisbet, R.M., Preuss, T.G., Hammers-Wirtz, M. and Grimm, V., 2013. Extrapolating ecotoxicological effects from individuals to populations: a generic approach based on Dynamic Energy Budget theory and individual-based modeling. *Ecotoxicology*, **22**: 574-583. https://doi.org/10.1007/s10646-013-1049-x

Meng, T., 2002. Studies on the feeding of anchovy (*Engraulis japonicus*) at different life stages on zooplankton in the middle and southern waters of the Yellow Sea. *Mar. Fish. Res.*, **24**: 1-9.

Nisbet, E.K., Zelenski, J.M. and Murphy, S.A., 2012. Happiness is in our nature: Exploring nature relatedness as a contributor to subjective well-being. *J. Happin. Stud.*, 1 303-322.

Ohshimo, S., 1996. Abundance estimation of biomass and school character of anchovy *Engraulis japonicus* in the East China Sea and the Yellow Sea. *Fish. Sci.*, **62**: 344-349. https://doi.org/10.2331/fishsci.62.344

Petitgas, P., Huge, H., Ro , D., Loizeau, V., Pecquerie, L. and Bacher, C., 2013. Responses of European anchovy vital rates and population growth to environmental fluctuations: an individual-based modeling approach. *Ecol. Model.*, **250**: 370-383. https://doi.org/10.1016/j.ecolmodel.2012.11.017

Pecquerie, L., Petitgas, P. and Kooijman, S.A., 2009. Modeling fish growth and reproduction in the context of the dynamic energy budget theory to predict environmental impact on anchovy spawning duration. *J. Sea Res.*, **62**: 93-105. https://doi.org/10.1016/j.seares.2009.06.002

Railsback, S.F. and Grimm, V., 2011. *Agent-based and individual-based modeling*: *A practical introduction*. Princeton University Press.

Regner, S., 1996. Effects of environmental changes on early stages and reproduction of anchovy in the Adriatic Sea. *Sci. Mar.*, **60**: 167–177.

Serpa, D., Ferreira, P.P., Ferreira, H., da Fonseca, L.C., Dinis, M.T. and Duarte, P., 2013. Modelling the growth of white seabream (*Diplodus sargus*) and gilthead seabream (*Sparus aurata*) in semi-intensive earth production ponds using the Dynamic Energy Budget approach. *J. Sea Res.*, **76**: 135-145. https://doi.org/10.1016/j.seares.2012.08.003

Shan, X., Li, X., Yang, T., Sharifuzzaman, S.M., Zhang, G., Jin, X. and Dai, F., 2017. Biological responses of small yellow croaker (*Larimichthys polyactis*) to multiple stressors: A case study in the Yellow Sea, China. *Acta Oceanolog. Sin.*, **36**: 39–47. https://doi.org/10.1007/s13131-017-1091-2

Sibly, R.M., Grimm, V., Martin, B.T., Johnston, A.S., Kułakowska, K., Topping, C.J. and DeAngelis, D.L., 2013. Representing the acquisition and use of energy by individuals in agent-based models of animal populations. *Methods Ecol. Evolut*., **4**: 151-161. https://doi.org/10.1111/2041-210x.12002

Smallegange, I.M., Caswell, H., Toorians, M.E. and Roos, A.M., 2017. Mechanistic description of population dynamics using dynamic energy budget theory incorporated into integral projection models. *Meth. Ecol. Evol.,* **8**: 146-154.

Sun, Y., Ma, Z.M., Liu, Y. and Tang Q.S., 2006. The gastric evacuation rate of anchovy (*Engraulis japonicus*) in different growth stages in Huanghai Sea and East China Sea (in Chinese with English abstract). *Acta Oceanolog. Sin*., **28**: 103-108.

Temminck, C.J. and Schlegel, H., 1846. Pisces, parts 5–6. In: *Fauna Japonica, sive descriptio animalium quae in itinere per Japoniam suscepto annis 1823–30 collegit, notis observationibus et adumbrationibus illustravit* (ed. P.F. de Siebold). Ludguni Batavorum, Leiden, pp 73–112.

Wan, R., Huang, D. and Zhang, J., 2002. Abundance [illegible] distribution of eggs and larvae of *engraulis japonicus* in the northern part of East China [illegible] and the southern part of Yellow Sea and its relationship with environmental conditions. *Shuichan Xuebao*, **26**: 321-330.

Wan, R.J., Li, X.S., Zhuang, Z.M. and Meng, Z.N., 2004. Experimental starvation on *Engraulis japonicus* larvae and definition of the point of no return. *J. Fish. China*, **28**: 7[illegible].

Wan, R. and Tian, X., 20[illegible]e variability and natural mortality dynamics of anchovy *Engraulis japonicus* eggs under high fishing pressure. *Mar. Ecol. Progr. Ser.*, **465**: 243-251. https://doi.org/10.3354/meps09795

Wang, R., Chen, Y.Q., Zuo, T. and Wang, K., 2003. Quantitative distribution of euphausiids in the Yellow Sea and East China Sea in spring and autumn in relation to the hydrographic conditions. *J. Fish. China*, **27**: 31-38.

Zhao, X.Y., 2006. *Population dynamic characteristics and sustainable utilization of the anchovy stock in the Yellow Sea*. Doctor Dissertation. Ocean University of China, Qingdao (In Chinese with English abstract).

Zhao, X., Wang, Y. and Dai, F., 2008. Depth-dependent target strength of anchovy (*Engraulis japonicus*) measured in situ. *ICES J. Mar. Sci*., **65**: 882-888. https://doi.org/10.1093/icesjms/fsn055

Zhao, X., Hamre, J., Li, [illegible] Jin, [illegible] and Tang, Q., 2003. Recruitment, sustainable yield and possible ecological consequences of the sharp decline of the anchovy (*Engraulis japonicus*) stock in the Yellow Sea in the 1990s. *Fish. Oceanogr*., **12**: 495-501. https://doi.org/10.1046/j.1365-2419.2003.00262.x

Zhi[illegible], Z., Fan[illegible]ong, M., Zhishan, Y. and Jie, H., 2002. Abundance and biomass of the benthic meiofauna in the spawning ground of anchovy (*Engraulis japonicus*) in the Southern Yellow Sea, China. *J. Ocean Univ. Qingdao*, **32**: 251-258.

Zhu, D., 1990. Anchovy and other fish resources in the Yellow Sea and East China Sea. *Mar. Fish. Res. China*, **11**: 1-143.

Zhu, D.S. and Iversen, S.A., 1990. Anchovy and other fish resources in the Yellow Sea and East China Sea. *Mar. Fish. Res*., **11**: 1-143 (in Chinese with English abstract).

Zhu, J.C., Zhao, X.Y. and Li, F.G., 2007. Growth characters of the anchovy stock in the Yellow Sea with its annual and seasonal variations. *Mar. Fish. Res*., **28**: 64-72.

Zuidema, P.A., Jongejans, E., Chien, P.D., During, H.J. and Schieving, F., 2010. Integral projection models for trees: a new parameterization method and a validation of model output. *J. Ecol*., **98**: 345–355. https://doi.org/10.1111/j.1365-2745.2009.01626.x